

Supporting Information

Rapid and Large-Scale Synthesis of Chiral and Fluorescent Sulfur Quantum Dots for Intracellular Temperature Monitoring

Li Zhao^{#1}, Tianjian Sha^{#1}, Yufu Liu², Qingsong Mei^{2}, Haibin Li¹, Pinghua Sun^{1,3}, Haibo*

Zhou^{1}, and Huaihong Cai^{4*}*

¹ College of Pharmacy, Jinan University, Guangzhou, Guangdong 510632, China; E-mail: haibo.zhou@jnu.edu.cn, pinghuasunny@163.com

² School of Medicine, Jinan University, Guangzhou, Guangdong 510632, China; E-mail: qsmei@jnu.edu.cn

³ Key Laboratory of Xinjiang Phytomedicine Resource and Utilization, Ministry of Education, School of Pharmacy, Shihezi University, Shihezi, Xinjiang 832003, China

⁴ College of Chemistry and Materials Science, Jinan University, Guangzhou, Guangdong 510632, China; E-mail: thhcai@jnu.edu.cn

Table of Contents

Figure S1. Pictures of SQDs and traditional SQDs under UV-light.	S-3
Figure S2. Fluorescent photograph of purified SQDs.....	S-3
Figure S3. The high-resolution N 1s spectrum of the SQDs.	S-4
Figure S4. Circular dichroism spectra of L- and D-cysteine.	S-4
Figure S5. UV-Vis absorption spectra.	S-5
Figure S6. The fluorescence spectra and circular dichroism spectra of Gly-SQDs.	S-5
Figure S7. PL spectra of the time stability of SQDs.....	S-6
Figure S8. PL spectra of SQDs dependent in different pH solution.	S-6
Figure S9. PL spectra of SQDs synthesized by using different concentrations of H ₂ O ₂	S-7
Figure S10. UV absorption spectra of SQDs obtained by different concentrations of H ₂ O ₂	S-7
Figure S11. PL spectra of SQDs obtained from different temperature.	S-8
Figure S12. PL spectra of SQDs obtained from different amount of L-Cysteine.	S-8
Figure S13. Plots of integrated PL intensity of SQDs and quinine sulfate as a function of optical absorbance at 350 nm.....	S-9
Table S1. Plots of integrated PL intensity of SQDs and quinine sulfate as a function of optical absorbance at 350 nm and relevant data.	S-9
Table S2. Five different circumstances about sulfur quantum dots synthesis.....	S-10
Figure S14. Temperature-dependent fluorescence intensity of SQDs.	S-11
Figure S15. Photos of the SQDs in different temperatures (20-50 °C) under UV-light.....	S-11
Figure S16. Temperature-dependent fluorescence after storage for 7 d and 14 d.	S-12
Figure S17. The fluorescence spectra and the calibration curves of fluorescence quenching efficiency within a range of 20-50 °C under different excitation wavelength.	S-13
Figure S18. Cell viability.	S-14
Figure S19. Confocal fluorescence images of Hela cells.....	S-14
Figure S20. Bright field images of Hela cells.....	S-15
Figure S21. Confocal fluorescent images (DAPI and SQDs) of Hela cells.	S-15
Figure S22. Temperature dependent fluorescence intensity in cell.	S-16
Figure S23. Temperature dependent calibrated quenching efficiency in cell.	S-17

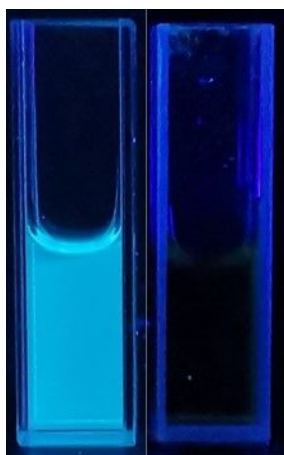


Figure S1. Picture of sulfur quantum dots under 365 nm UV-light through this method (Left).
Picture of sulfur quantum dots synthesized by PEG-400-based traditional method (right).



Figure S2. Fluorescent photograph of purified sulfur quantum dots for a patch of experiment.

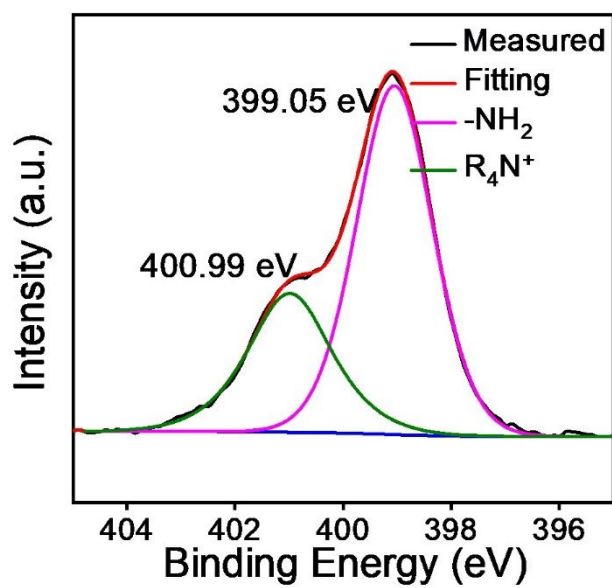


Figure S3. The high-resolution N 1s spectrum of the sulfur quantum dots.

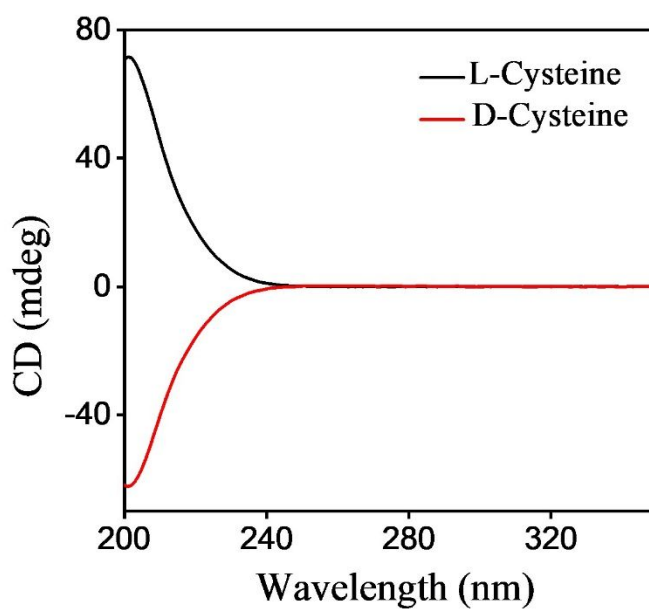


Figure S4. Circular dichroism spectra of L- and D-cysteine.

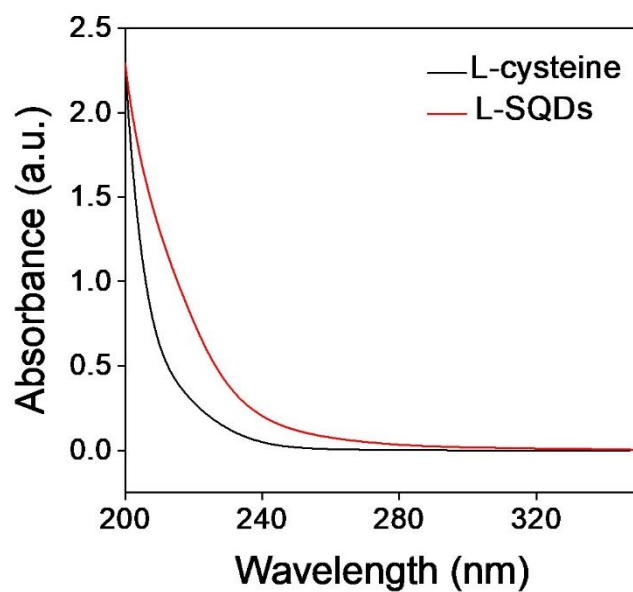


Figure S5. UV-Vis absorption spectra of the L-cysteine and L-sulfur quantum dots.

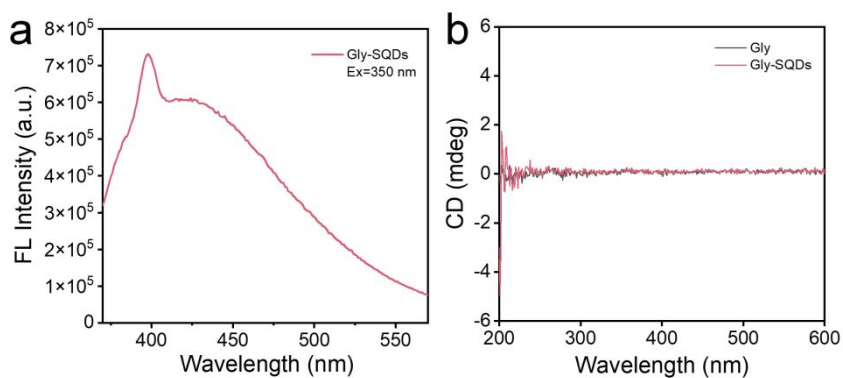


Figure S6. (a) The fluorescence spectra of Glycine-SQDs. (b) The Circular dichroism spectra of Glycine and Glycine-SQDs.

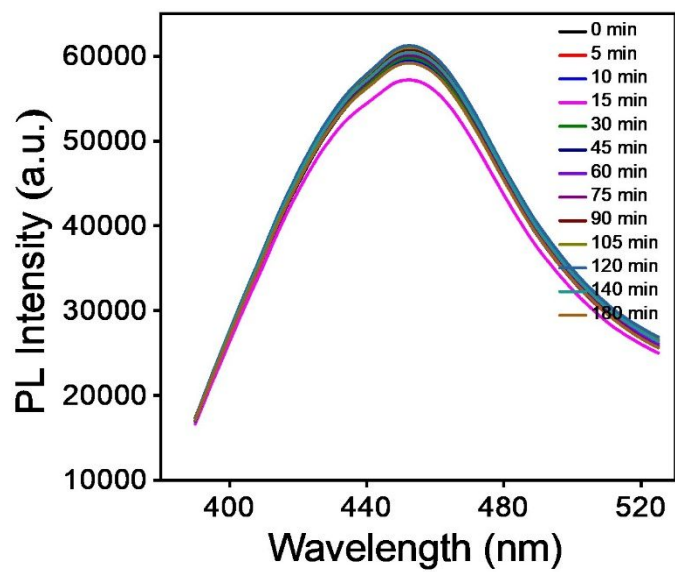


Figure S7. PL spectra of the time stability of sulfur quantum dots.

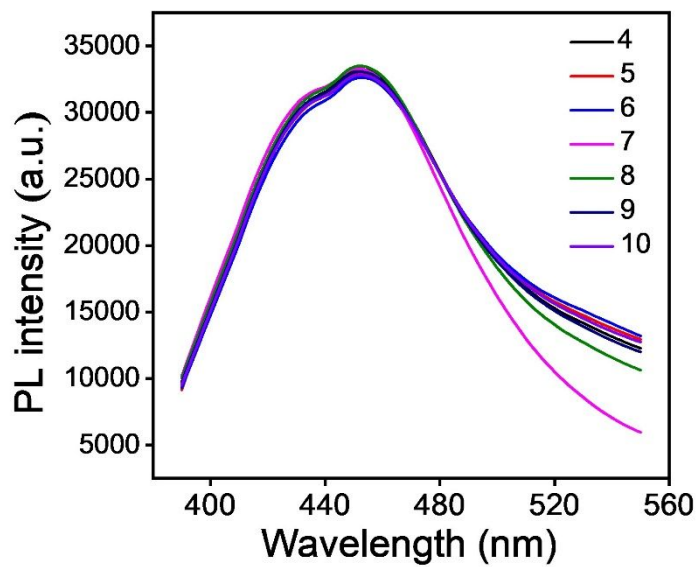


Figure S8. PL spectra of sulfur quantum dots dependent in different pH solution.

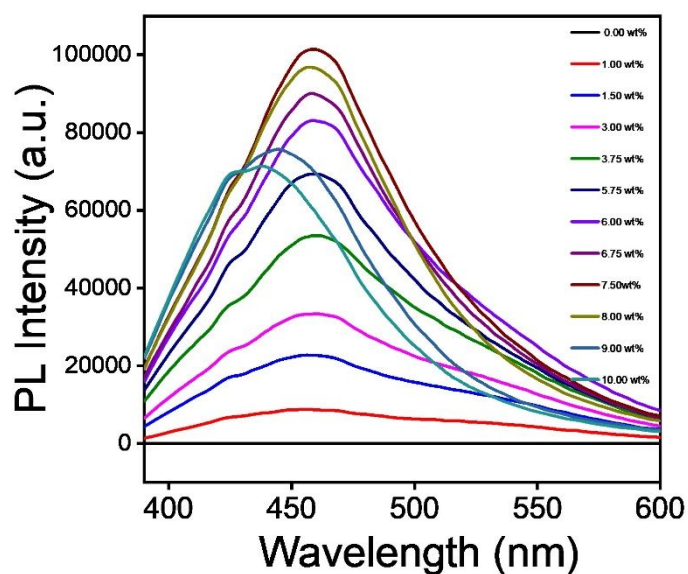


Figure S9. PL spectra (excited at 370 nm) of sulfur quantum dots synthesized by using different concentrations of H_2O_2 .

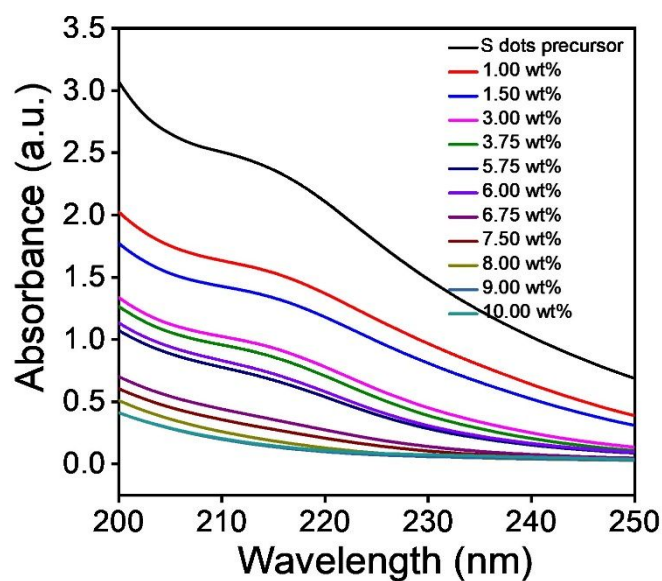


Figure S10. UV absorption spectra of sulfur quantum dots synthesized by adding different concentrations of H_2O_2 .

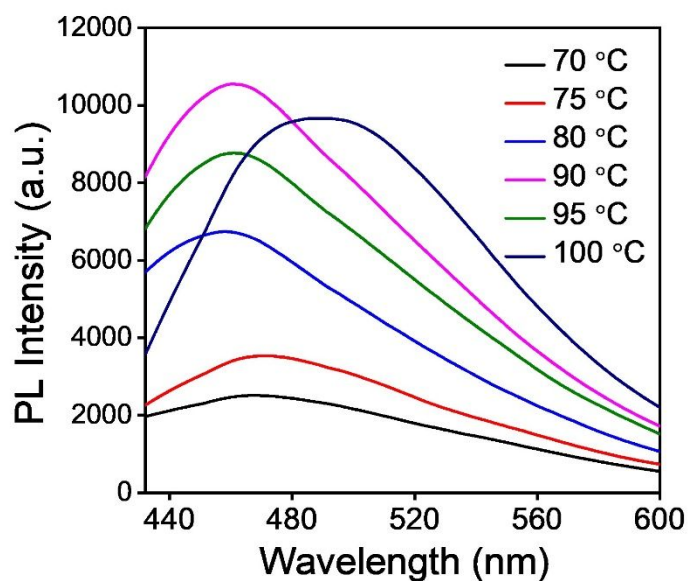


Figure S11. PL spectra of sulfur quantum dots obtained from the reaction heated to different temperature, and other conditions are: 0.7 g sublimed sulfur power, 2.1 g L-Cysteine, 2.1 g NaOH and 35 mL water.

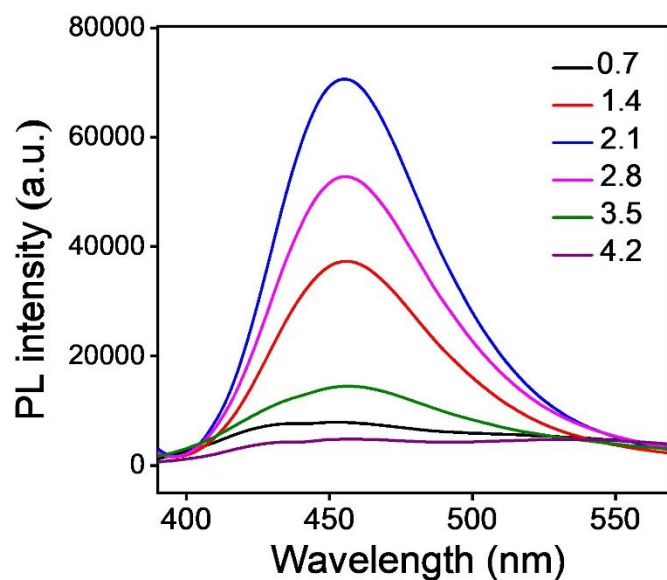


Figure S12. PL spectra of sulfur quantum dots obtained from the reaction using different amount L-Cysteine, and other conditions: 0.7 g sublimed sulfur power, 2.1 g NaOH, 35 mL water and 90 °C reaction temperature

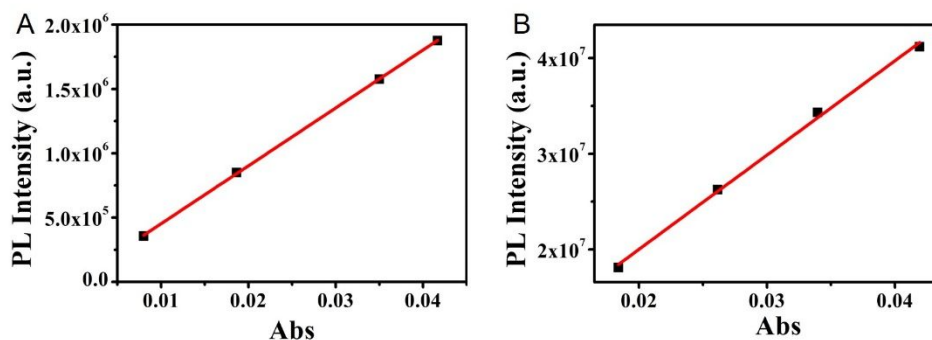









Figure S13. Plots of integrated PL intensity of SQDs and quinine sulfate as a function of optical absorbance at 350 nm.

Table S1. Plots of integrated PL intensity of SQDs and quinine sulfate as a function of optical absorbance at 350 nm and relevant data.

Sample	Abs	PL Intensity	Slope (I/A)	QY	
SQDs	1	0.042	1.88×10^6	4.50×10^7	2.51%
	2	0.035	1.58×10^6		
	3	0.019	8.50×10^5		
	4	0.008	3.57×10^5		
Quinine Sulfate	1	0.042	4.12×10^7	9.85×10^8	55%
	2	0.034	3.43×10^7		
	3	0.026	2.63×10^7		
	4	0.018	1.81×10^7		

Table S2. Five different circumstances about sulfur quantum dots synthesis. Sample 1: precursor contained sulfur powder, NaOH and cysteine. Then, added H₂O₂ into precursor. Sample 2: precursor contained sulfur powder, NaOH and PEG-400. Then, added H₂O₂ into precursor. Sample 3: precursor contained sulfur powder and NaOH. Sample 4: precursor contained cysteine and NaOH. Sample 5: precursor contained sulfur powder and cysteine. Step 1 synthesis conditions: 90 °C stirred under atmosphere for 10 min. Step 2 synthesis conditions (sample 1 and sample 2): 7.5% H₂O₂ dropped into the precursor with vigorously stirring under atmosphere (volume ratio of precursor to H₂O₂ is 4:3).

Sample number	Step 1				Step 2		
	Precursor				Phenomenon	H ₂ O ₂	Phenomenon
	Sulfur	NaOH	Cysteine	PEG-400			
1	√	√	√			√	
2	√	√		√		√	
3	√	√					
4		√	√				
5	√		√				

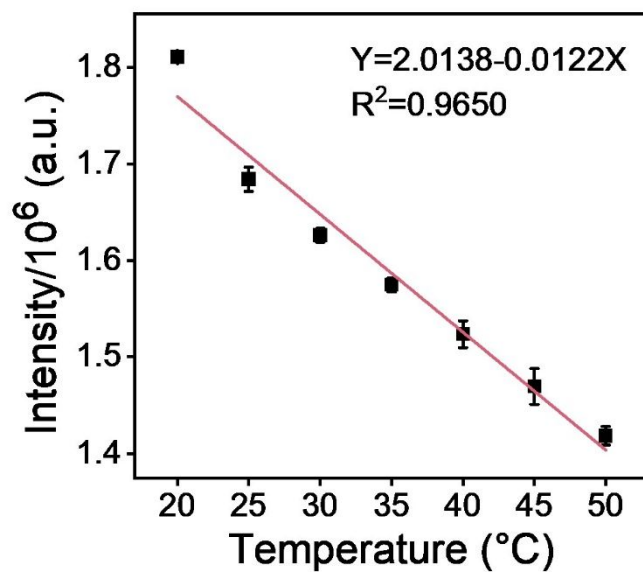


Figure S14. Temperature-dependent fluorescence intensity of SQDs in water within a range of 20-50 °C.



Figure S15. Photos of the SQDs in different temperatures (20-50 °C) under UV light.

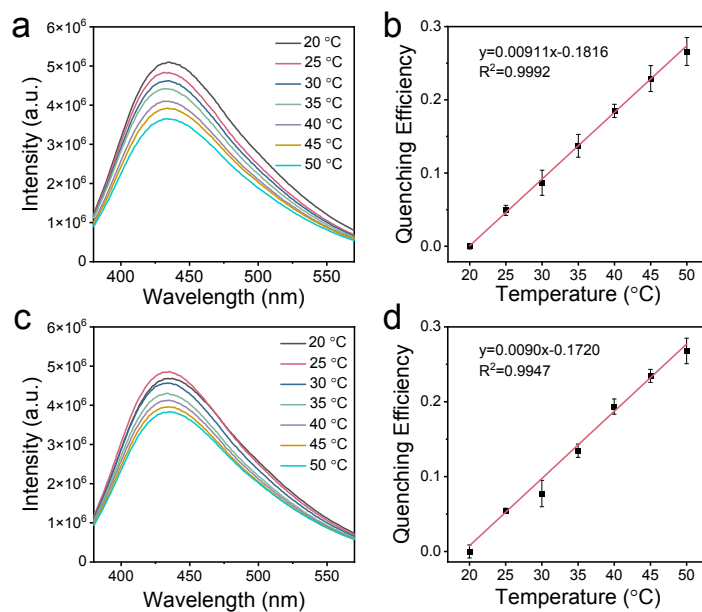


Figure S16. Temperature-dependent fluorescence variations and the quenching efficiency linear calibrations of SQDs aqueous solution within a range of 20-50 ° C after storage for 7 d (a and b) and 14 d (c and d).

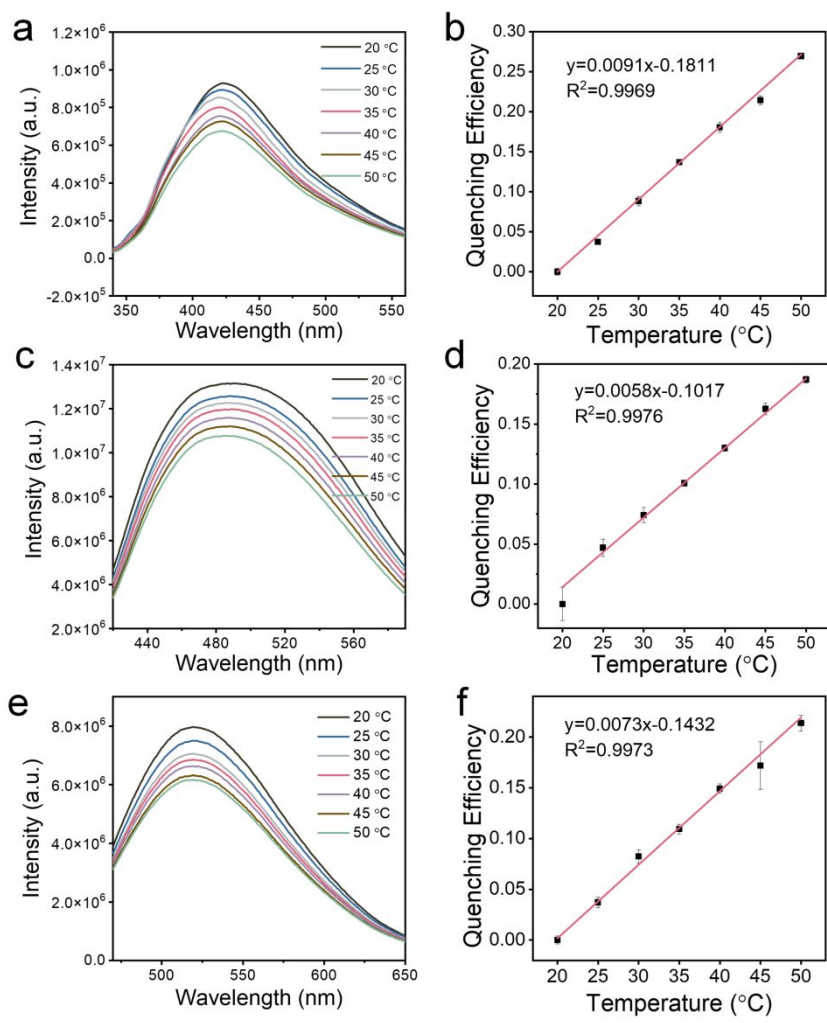


Figure S17. The fluorescence spectra and the calibration curves of fluorescence quenching efficiency within a range of 20-50 °C under different excitation wavelength. (a and b) Ex=325 nm, (c and d) Ex=400 nm, (e and f) Ex=450 nm.

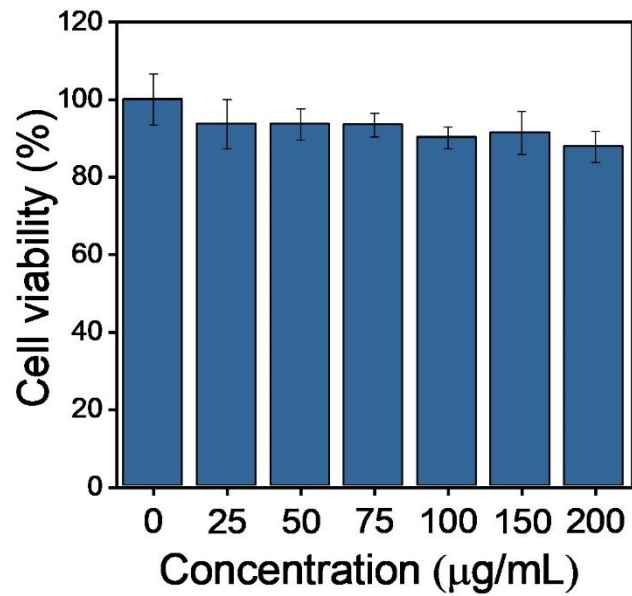


Figure S18. Cell viability of HeLa cells incubated with different concentrations of SQDs.

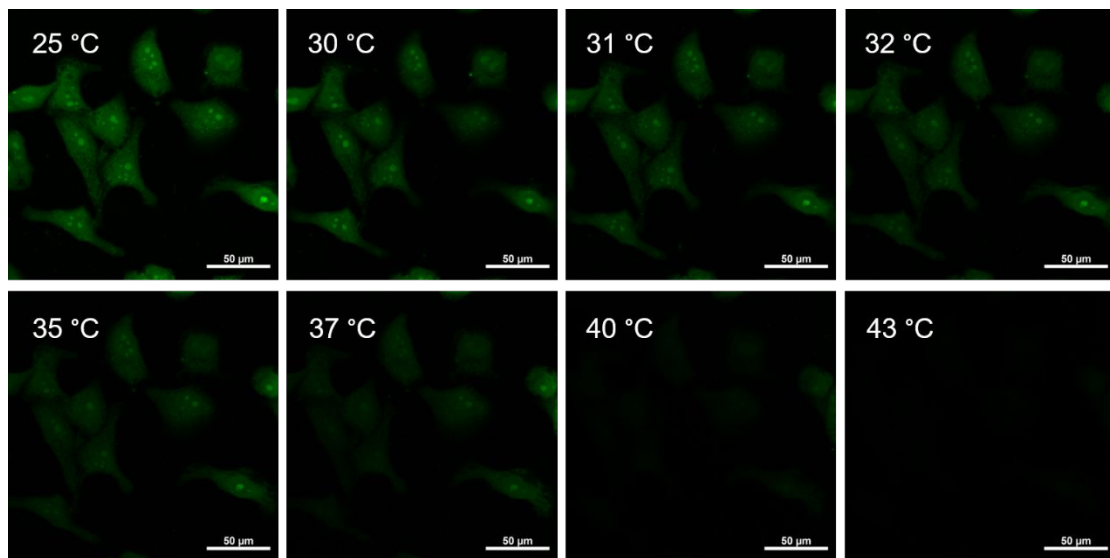


Figure S19. Confocal fluorescence images of HeLa cells obtained in the temperature range of 25 °C to 43 °C (Scale bar: 20 µm).

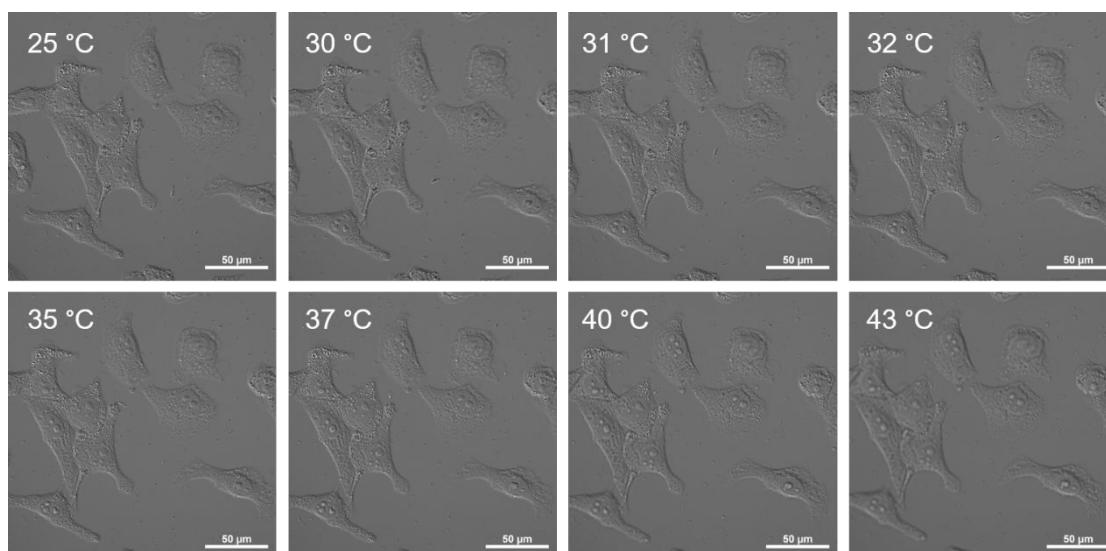


Figure S20. Bright field images of HeLa cells obtained in the temperature range of 25 °C to 43 °C (Scale bar: 20 μm).

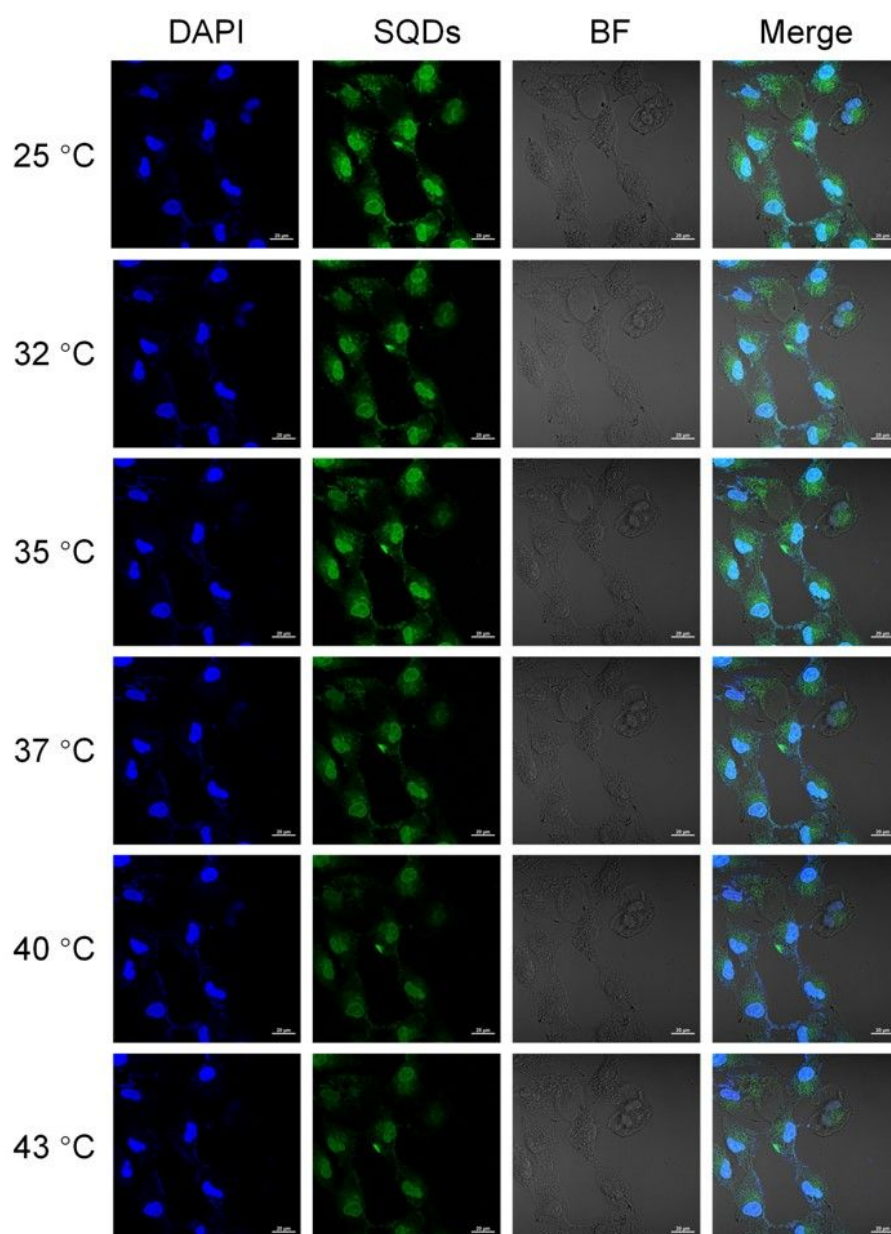


Figure S21. Confocal fluorescent images of HeLa cells obtained at different temperatures.

Scale bars are 20 μm .

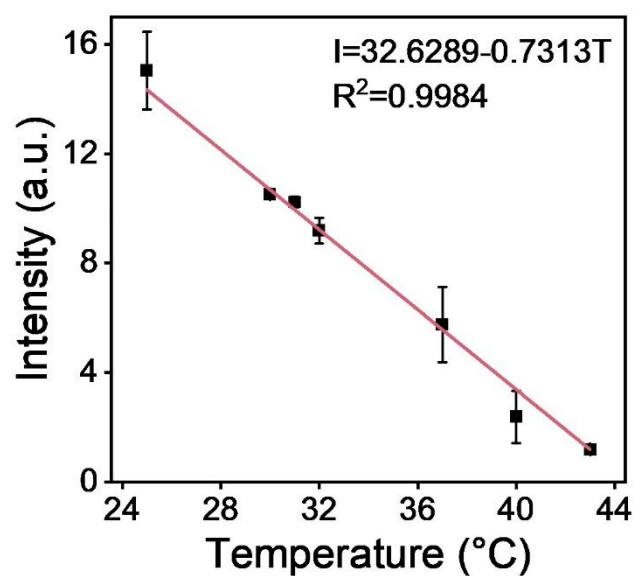


Figure S22. Temperature dependent calibration curve of fluorescence intensity in cell (25 °C-43 °C).

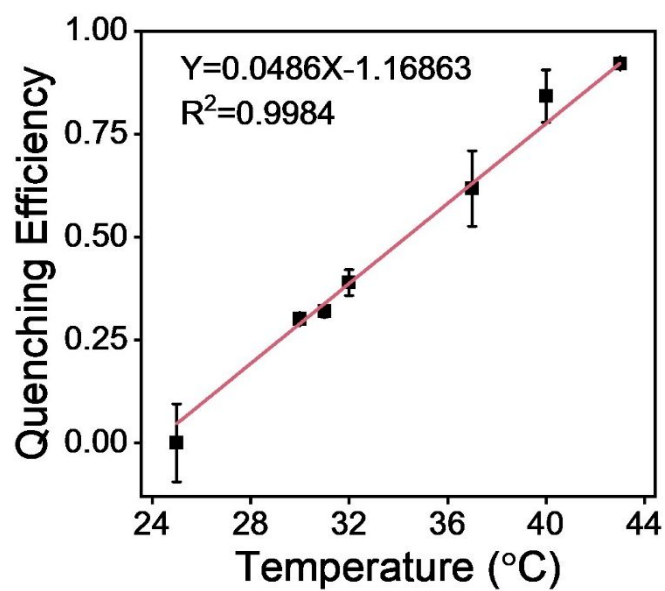


Figure S23. Temperature dependent calibration curve of fluorescence quenching efficiency in cell (25 °C-43 °C).